Journal of Applied Sciences

ISSN 1812-5654

science alert

ANSInet
an open access publisher
http://ansinet.com

Journal of Applied Sciences 8 (3): 420-431, 2008
ISSN 1812-5654

Numerical Analysis of Slab-Column Connections Strengthened with Carbon Fiber Reinforced Polymers

A. Kheyroddin, S.R. Hoseini Vaez and H. Naderpour
Engineering Faculty, Semnan University, Semnan, P.O. Box 35195-363, Iran

Abstract: This study presents nonlinear finite element analysis of slab-column connection in order to investigate the effect of using CFRP (Carbon Fiber Reinforced Polymer) sheets on their structural behavior. Verification of study needs to calibrate the un-strengthened analytical models by available experimental data. In this case two groups of models with three layers of Solid 65 elements throughout the depth of the slabs were analyzed. One of them was consisted of the smeared reinforcement throughout the entire slab which indicated a reasonably accurate simulation of the load-deflection curves with a steel volume ratio of 0.028 and also gives a good indication of the cracking behavior of the slabs. In the other group, smeared reinforcement located at bottom layer was used. In both groups the pre-cracking branch of the different curves follows the experimental results very closely. Beyond cracking, the models of last group defined appear stiffer. The punching truncated pyramid of control model is in a very close agreement with the experiment. Slab model by using CFRP plates introducing to program by Solid 46 elements, have been analyzed. Results indicated that final deflection of slab has been increased of 36% while strength of the slab has been increased slightly. Also, strengthening of slab with increasing steel volume ratio in the central zone affects on behavior of the slabs with an increase in both, the final load and deflection.

Key words: Composite, CFRP, nonlinear, slab-column connections, finite element, strengthening

INTRODUCTION

Concrete flat slab floors provide an elegant form of construction, which simplifies and speeds up site operations, allows easy and flexible partition of space and reduces the overall height of buildings. However, flat slab construction is not ideal from the structural point of view, because of the high shear stresses around supporting columns, which can lead to abrupt punching shear failure at a load which is well below its flexural strength. The problem with this failure mode is that it is brittle and catastrophic due to the inability of the concrete to support the large tensile stresses that developed. This failure occurs with the potential diagonal crack following the surface of a truncated cone or pyramid around the column. The failure surface extends from the bottom of the slab, at the support, diagonally upward to the top surface. The angle of inclination with the horizontal depends upon the nature and amount of reinforcement in the slab. It may range between about 20 and 45° (Nilson *et al*., 2003). It is obvious, that in design, attention should be given to both strength and ductility when punching shear is being considered.

Although there is a great amount of experimental data available on punching shear failure of slabs, there has been little success in developing a universal theoretical model to predict the behavior of an arbitrary concrete structure (Vidosa *et al*., 1991). The American Society of Civil Engineers had presented an extensive review of the underlying theory and the application of the finite element method to the linear and nonlinear analysis of reinforced concrete structures in a state-of-the-art report (ASCE, 2002). It was stated that the results from the finite element analysis significantly relies on the stress-strain relationship of the materials, failure criteria chosen, simulation of the crack of concrete and the interaction of the reinforcement and concrete. The nonlinear stress distribution in the connection is not clearly understood. Several previous attempts (Malvar, 1992; Marzouk and Chen, 1993; Marzouk and Jiiang, 1996; Polak, 1998) have been focused on prediction of the slabs failure in punching shear using various finite element models. The models presented in this paper, were developed specifically to model the behavior of the experimental specimen.

The trend towards lighter and more flexible construction configurations led to increased usage of flat

Corresponding Author: Hosein Naderpour, No. 4, Roshan Alley, Bastan St., Jomhouri Ave., Tehran, Iran
Tel: +98-21-66916238 Fax: +98-21-88013876

plate construction in 1950s. Reinforced concrete flat plate construction has been used as an economical structural system for many buildings. In high seismic regions, flat plate structures are supplemented with either a moment frame or shear wall lateral resisting system. Today, ductile detailing for all structural connections, including for those which are gravity load only, is a principal concept that was learned initially as a result of the failures observed during the 1971 San Fernando earthquake (FEMA, 1997). All the gravity load only slab column connections in a flat plate structure must maintain their capacity at the maximum displacement of the lateral system. During this lateral deformation, the brittle failure mode of slab punching can occur. A punching shear failure, generated by the combination of the gravity loading and seismically induced unbalanced moment in the slab, can occur with little or no warning and has resulted in the progressive collapse of these types of structures. In the 1985 Mexico City earthquake, 91 flat plate buildings collapsed and 44 were severely damaged due to punching failure (Ghali and Megally, 2000). Prior to the ACI (American Concrete Institute) code revisions in the 1970s, which began to reflect ductile detailing lessons learned, reinforcing for flat slab systems did not require continuity of top and bottom reinforcement. Top reinforcing, used for negative bending, could be completely curtailed away from the column supports. Bottom reinforcing was only required to extend into supports by 150 mm (6 inches). It is now well known that positive bending can occur at the face of supports during lateral displacements inducing a bond failure at these short embedment locations. Due to the inadequacies of the pre-1971 design codes, there is a need to understand the behavior of the structures designed to these codes and to develop ways to upgrade these structures to provide an acceptable level of seismic safety.

Previous studies have been performed on repair techniques for damaged ductile slab-column connections using steel plates and through-bolting (Farhey *et al*., 1995). This technique could also be used to upgrade the performance of non-ductile connections, however, the aesthetic impact to the existing structure is a potential drawback.

In recent years, use of fiber reinforced polymer composites for concrete structures has been on the rise. Despite the relatively high cost of the CFRP material, its high strength-weight ratio, high resistance to corrosion and easy handling and installation have made CFRP the material of choice in an increasingly large number of projects where increased strength or inelastic deformation capacity (ductility), or both, must be achieved for seismic retrofitting (Triantafillou, 2003).

The bulk of the work, presented in this study, focuses on numerical models developed to predict the response of the slab including the load-deflection behavior, the ultimate failure load and the crack pattern; this preliminary modeling is necessary to be considered as the basis of the main study including strengthening of slabs by using CFRP composites. Three-dimensional nonlinear finite element models were created to simulate the behavior of the flat slab by using the computer code ANSYS (ANSYS, 2004). The models are based on an eight-node isoparametric element. A parametric study was carried out to look at the variables that can mainly affect the behavior of the models.

Construction and verification of finite element static model

Experimental specimen: Internal connections having shapes of square, rectangular or circular specimens with edges simply supported and free to lift and centrally loaded through a column stub raise questions in the following respects: 1- The boundary conditions in the model are different to those of the actual structure, 2- The redistribution of moments around the column in the test specimen is different from a real structure (Desayi and Seshadri, 1997). However, work carried out by Gardner and Shao (1996) demonstrated that the isolated punching shear tests can represent the punching shear behavior of interior slab-column connections in continuous slab systems.

Slab specimen P0A tested by Kruger *et al*. (1998) was selected for the numerical analysis (Fig. 1). The experimental slab-column connection was full scale model. The boundaries of the specimen were selected at the position of the line of contraflexure so as to contain the hogging moment region around the column. The specimen support was considered as a simple support during the test on knife edges fixed on steel beams so that the edges are free to lift. The test set-up and loading arrangement are shown in Fig. 1. The specimen was $3000\times3000\times150\,mm^3$. The cylinder compressive strength of the concrete f'_c was 35 MPa. The mean ratio in each direction of the flexural reinforcement ρ was 1.0% for the slab. The specimen was inversely placed. The testing arrangement was convenient for both loading and inspecting the slab for cracking during the test. The vertical load was applied centrally through the column stub, with the slab specimen simply supported along four edges to simulate an inverted isolated slab-column connection. The load was applied monotonically using a hydraulic jack set by deflection control. Readings were taken at 40 kN intervals.

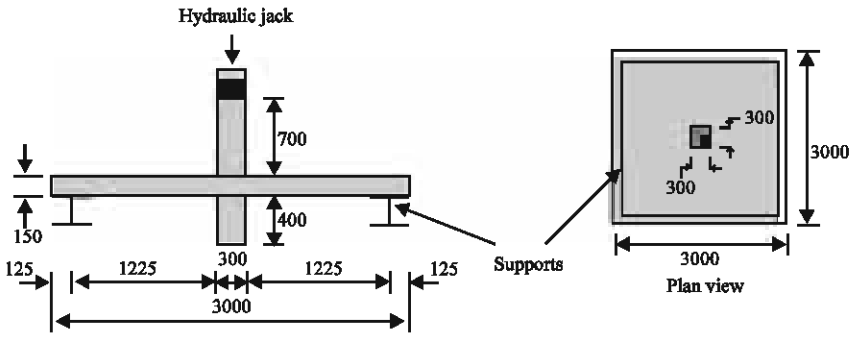

Fig. 1: Test set-up and specimen (dimensions in mm)

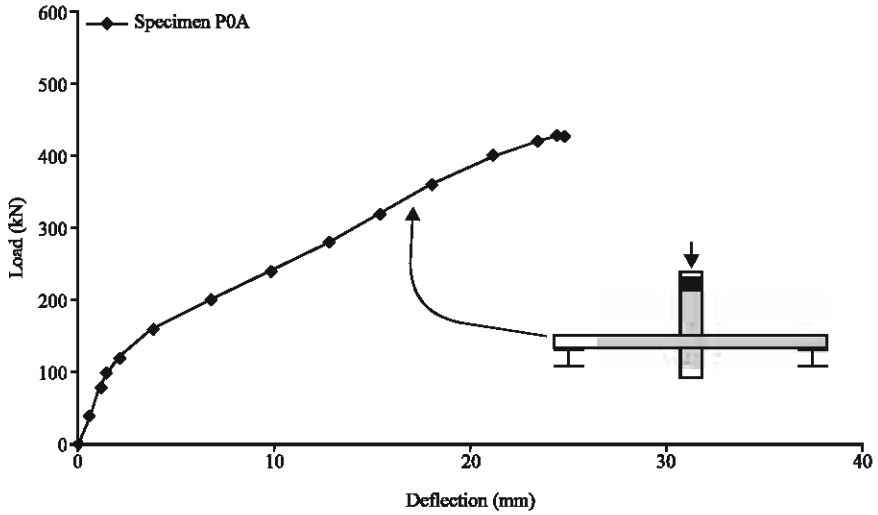

Fig. 2: Load versus maximum vertical slab deflection

Figure 2 shows the maximum slab deflection versus the load applied by the hydraulic jack. The specimen behaved linearly from the initial loading up to the occurrence of the first crack. The first crack appears between the second and the third load step at approximately 100 kN. The slab on reaching the peak load (423 kN) failed in a brittle manner with a sudden loss of capacity by punching, indicating very low ductility and residual strength. Failure for this slab can be defined as punching shear failure on account of the fact that the load quickly dropped when failure was reached as shown in Fig. 2.

Finite element modeling of slab-column connections: In previous years some numerical tests were carried out applying the finite element method. Among these, studies with two-dimensionally modeled systems with rotationally symmetrical elements (Hallgren, 1996; Menétrey, 1994) must be distinguished from the purely three dimensional, idealized systems. A separate position is assumed by tests applying degenerated shell elements which are placed in layers (Polak, 1998). The three-dimensional idealization offers the option of defining and modeling various characteristics in any direction and the three-dimensional model is also highly suitable for observing the formation of punching cracks and their position in the slab.

In this study, it was decided to focus on modeling both the load-deflection characteristics of the slabs and also the initial onset of cracking. The experimental data that was obtained in a comprehensive study (Kruger *et al*., 1998), described above, was used as a comparison with the numerical results. The ANSYS finite element package was used to carry out the modeling and the Solid 65 element used to model the concrete. The Solid 65 element is a three-dimensional isoparametric element, capable of cracking in tension and crushing in compression. The ANSYS element (ANSYS, 2004) is defined by eight nodal points each having three translational degrees of freedom x, y and z (and no

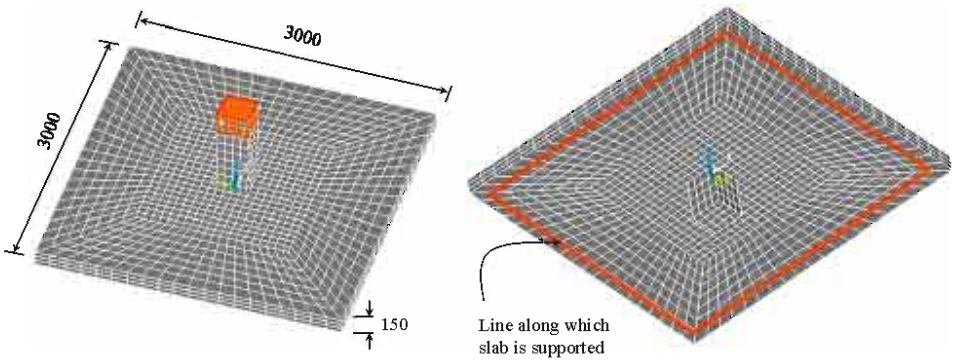

Fig. 3: Numerical model (dimensions in mm)

rotations), along with a 2×2×2 Gaussian integration scheme which is used for the computation of the element stiffness matrix. The model is also capable of simulating the interaction between the two constituents, concrete and reinforcement. Thus, it can be used to describe the behavior of the reinforced concrete material. The element has one solid material and up to three different reinforcing bars material properties can be defined. The most important feature of this element is that it can represent both linear and nonlinear behavior of the concrete. For the linear stage, the concrete is assumed to be an isotropic material up to cracking. For the nonlinear part, the concrete may undergo plasticity and/or creep.

The load is iterated step by step using the Newton-Raphson method. As was already stated, the slabs were simply supported along four sides, as shown in Fig. 3. Therefore the boundary conditions are quite simple to set-up. One corner had all translational degrees of freedom fixed, while one corner was fixed with two degrees of freedom so as to prevent the slab from moving and rotating in its own plane. The edges of the slab were not restrained as in the experimental set-up (Fig. 3).

In the static analysis, the stress-strain relations of concrete are modified to represent the presence of a crack. A plane of weakness in a direction normal to the crack face and a shear transfer coefficient β_t (represents conditions of the crack face) are introduced in the Solid65 element. The shear strength reduction for those subsequent loads, which induce shear across the crack surface, is considered by defining the value of β_t. This is important to accurately predict the loading after cracking, especially when calculating the strength of concrete member dominated by shear, such as slabs. The value β_t ranges from 0.0 to 1.0, with 0.0 representing a smooth crack (complete loss of shear transfer) and 1.0 representing a rough crack (no loss of shear transfer) (ANSYS, 2004). The value of β_t used in many studies of reinforced concrete structures, however, varied between 0.05 and 0.25 (Bangash, 1989; Hemmaty, 1998; Huyse *et al*., 1994). A number of preliminary analyses were attempted in this study with various values for the shear transfer coefficient within this range, but convergence problems were encountered at low loads with β_t less than 0.2. Therefore, the shear transfer coefficient used in this study was equal to 0.2.

The density γ and the Poisson's ratio ν of concrete were assumed as 2400 kg m^{-3} and 0.2. The shear transfer coefficient for a closed crack β_c was taken as 0.9. The ultimate uniaxial compressive strength f'_c introduced to the program was based on the experimental results (Kruger *et al*., 1998).

Newton-Raphson equilibrium iterations were used for nonlinear analysis. A displacement controlled incremental loading was applied through a column stub. This was used to simulate the actual loading used in the experimental program. Small initial load steps were used for detecting the first crack in the connections. Then, automatic time stepping was used to control the load step sizes. Line search and the predictor-corrector methods were also used in the nonlinear analysis for accelerating the convergence. The failure of the connection was defined when the solution for a small displacement increment did not converge. Consequently, the finite element model was constructed following the above-mentioned assumptions and considerations.

The main focus of these analyses is to model the load-deflection behavior of the specimen P0A that was given above. The numerical models were developed in two different groups. One of these groups consisted of three layers of elements in the depth of the slab with smeared reinforcement throughout (Fig. 4) and about the other, just for the bottom layer, smeared reinforcement defined (Fig. 5).

As stated already, a parametric study is presented in the following sections. This study was carried out to look at the effect of the volume of smeared reinforcement on

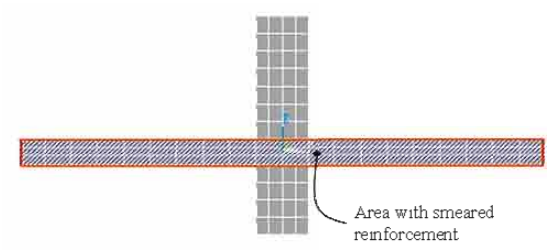

Fig. 4: All layers with smeared reinforcement

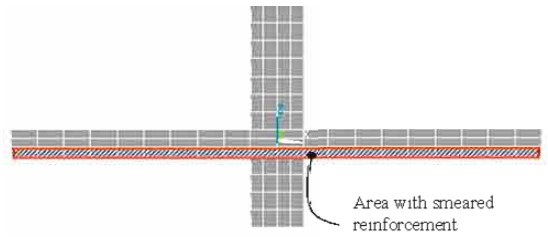

Fig. 5: Bottom layer with smeared reinforcement

the behavior of the slab. It is possible to establish the relationship between the volume ratio and section area of the reinforcement. However, the problem with specifying a volume of smeared reinforcement in a three-dimensional analysis is that, it is very difficult to relate the volume directly to the cross-sectional area of reinforcement present in the experimental specimen. Calculating the volume ratio to the section area ratio of the reinforcement for the shapes of solid elements generated is difficult. If the mesh under consideration is uniform with cubic elements throughout this relation is simple, the cross-sectional area being exactly equal to the volume specified.

Uniform mesh with cubic elements was used in preliminary analyses but the results didn't have accuracy. In the finite element of concrete structures, it is important to select an appropriate mesh size to meet the requirement of accuracy and computation speed; however, considering the mesh layout used in the present models was the same and is shown above in Fig. 3. The density of the mesh was increased under the area of loading and gradually reduced towards the edges of the slab. Therefore, as the mesh was not uniform, it was necessary to carry out a parametric study and look at the effect of the volume of smeared reinforcement present. This problem does not occur in the discrete reinforcement modeling currently being conducted.

Verification of the finite element model against experimental data

Group I: All layers with smeared reinforcement: This group of models consisted of three layers of elements in the depth with smeared reinforcement throughout the slab (Fig. 4). This group was investigated to look at the influence of the volume ratio of smeared reinforcement. The problem with using the smeared reinforcement option was that it tended to stiffen the element. Therefore, it was decided to carry out a parametric study to look at the effect of different values of the steel volume ratio.

Looking at the curves for the numerical models, the first thing one should note is that the behavior of all the models is exactly the same before cracking and the difference in behavior only occurs after initial cracking. Cracking of the models seems to occur at the same load as the experimental specimen, approximately 100 kN. If the curve for the first numerical model, SVR = 0.045 (SVR = Steel Volume Ratio), is studied, one can see the effects of a high volume of reinforcement on the behavior of the element. The element is quite stiff and therefore, there is significantly less deflection than the experimental specimen. The model also fails at a much greater load than the experimental specimen. As the volume ratio of reinforcement is reduced, the approximation of the load-deflection curve obtained using the models is improved. From the load-deflection curves below (Fig. 6), it seems that a steel volume ratio of 0.028 is the optimum value to achieve a good approximation of the experimental curve.

Group II: Bottom layer with smeared reinforcement: In this set of numerical models, the slab was divided into two parts: 1- a bottom layer consisting of Solid 65 elements with smeared reinforcement and 2- a top and middle layer consisting of Solid 65 elements without any smeared reinforcement (Fig. 5). The load-deflection curves for this set of models show a similar trend as obtained before (Fig. 7). The element is still quite stiff for higher values of smeared reinforcement. The best load-deflection curve is obtained at a value of 0.041. Cracking occurs in all the models at the same load and at a value slightly higher than previous models, 110 kN approximately.

Comparison of load-deflection curves: The load-deflection curves for the best model taken from each of the groups are compared below (Fig. 8). On examination of the plots, it is obvious that the best approximation is given by group I. For these slabs high volume ratios, such as 0.045, increase the stiffness of the elements considerably and an optimum volume ratio of 0.028 was found to give the best approximations of the load-deflection curve for the experimental specimen. It should be noted that this value was approximately three times more than the percentage of main steel in the experimental specimen, which indicates the influence of geometry of volume mesh. It was noticed that for similar values of the

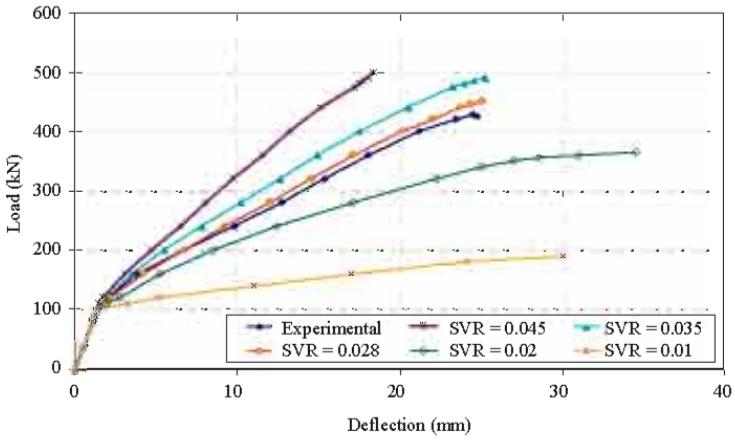

Fig. 6: Load-deflection curves for slabs of group I (SVR= Steel Volume Ratio)

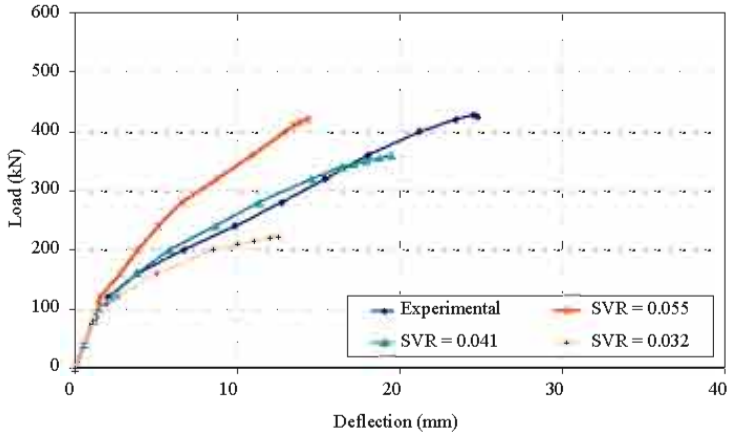

Fig. 7: Load-deflection curves for slabs of group II (SVR= Steel Volume Ratio)

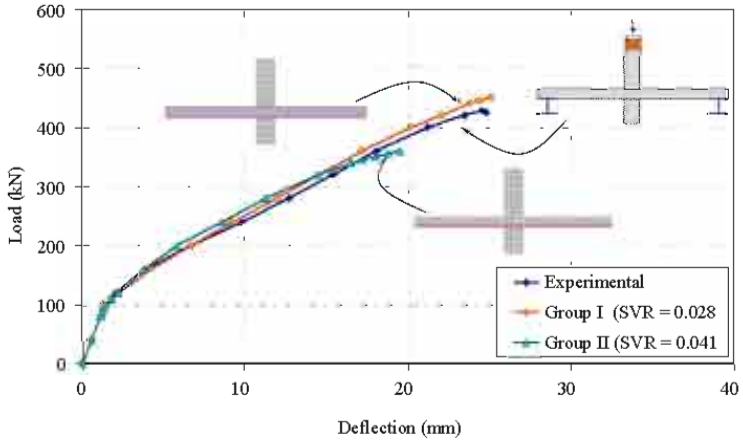

Fig. 8: Comparison of load-deflection curves for experimental and the best analytical models (SVR= Steel Volume Ratio)

reinforcement volume ratio in the bottom layer, the deflection of the slabs decreased and the final load supported by the slab also decreased. Similar results were noticed in the case of group I, slabs, where the load-deflection curves for the models are not as good approximations as those obtained using group I models.

Cracking pattern: Cracking may take place up to three orthogonal directions at each integration point. A crack may develop in one plane and if subsequent stresses tangential to the crack face are large enough, a second (or 3rd) crack will develop. An individual crack is treated as a smeared band of cracks. Cracks are defined by a combination of an angle θ in the xy plane and ϕ in the three dimensional space. The main advantages of the smeared crack approach compared to the discrete crack formulation is that 1- no predetermination of the location and orientation of the crack planes are necessary and 2- the original topology of the finite element mesh is maintained during cracking (Dyngeland *et al*., 1994). This can provide the useful information for crack modeling when discrete crack model is chosen at the later research program. Crushing failure assumes complete deterioration of the structural integrity of the concrete, such as spelling.

The smeared crack indicates a crack pattern similar to the experimental specimen. The first cracks opened up on the lower surface of inverted model in the form of flexural cracks near the column around 100 kN. After 100 kN, cracks propagated from the middle outwards and reached the slab edges. Subsequently, with increasing loads, more cracks occurred and advanced radially from the column faces towards the slab edges along the four axes of symmetry of the slab (central X and Y axes and two diagonals). Cracks parallel to the X and Y axes opened up at a lower load, less than 240 kN (Fig. 9, 10), whilst the cracks parallel to diagonal axes opened up at a load greater than 240 kN (Fig. 11). Figure 9, 10 and 11 shows crack pattern of modeling at first loading increments in comparison with the figure given by Ajdukiewice and Starosolski (1990).

By the time the load increment reached approximately 320 kN, only a few new diagonal cracks occurred and most of the cracks had already formed. After that, with increasing load, the width of the cracks close to the column increased substantially. In the period just prior to failure, the smeared cracks were formed from the connection area edges at upper surface of inverted model to the corners of the slab on the lower surface (Fig. 12). Also a circular stress concentration was formed around the loaded area indicating a punching shear type failure. The punching truncated pyramid is in a very close agreement with the experiment. Figure 12 shows a crack pattern of the model at a period just prior to ultimate load with elimination of radial cracks in comparison with the figure given by Ajdukiewice and Starosolski (1990).

Parametric study

Slab strengthening with increasing steel volume ratio in the central zone: The parametric study is carried out on the already observed control model of the slab. In this context the influence of strengthening the slab in the central zone with increasing steel volume ratio is investigated. In this case, the steel volume ratio in the central zone of the model increased up to 30 % compared to the control model. The steel volume ratio for central zone of strengthened model was 0.0364 and for peripheral zone was 0.028. Figure 13 shows the strengthened model curve against the control model curve and slab model curve with steel volume ratio of 0.035. On examination of the plots, it is obvious that the curve slope for the strengthened model is higher than the other curves and the deflection of the strengthened slab model increased and the final load supported by the strengthened slab also increased. The curves indicate that increasing the steel volume ratio in the central zone of the slab improves the behavior of the slabs.

Slab strengthening by CFRP

Carbon fiber reinforced polymers: Several techniques are currently available to retrofit and strengthen buildings with insufficient stiffness, strength and/or ductility. While these techniques are effective in improving the earthquake resistance of a building, they may add significant weight to the structure and thus alter the magnitude and distribution of the seismic loads. Also, the existing techniques are generally very labor intensive. Fiber reinforced polymers are composite materials consisting of high strength fibers immersed in a polymer matrix. The fibers in an FRP (Fiber Reinforced Polymer) composite are the main load-carrying element and exhibit very high strength and stiffness when pulled in tension. An FRP laminate will typically consists of several million of these thin, thread-like fibers. The polymer matrix protects the fibers from damage, ensures that the fibers remain aligned and allows loads to be distributed among many of the individual fibers in the composite (Kheyroddin and Naderpour, 2006).

Finite element modeling of strengthened connection: Here, the effectiveness of slab strengthening by CFRP in the central zone would be investigated. A layered solid element, Solid 46, was used to model the FRP composites. The element allows for up to 100 different

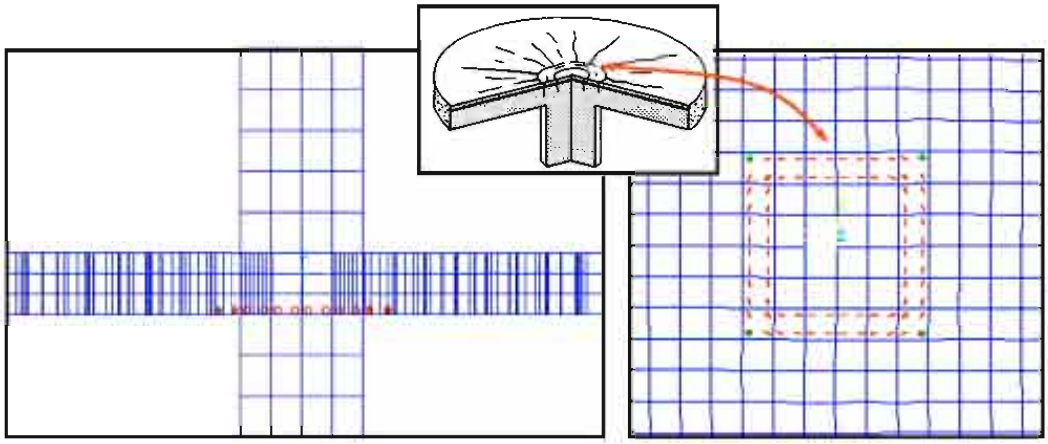

Fig. 9: Crack pattern at first loading increments

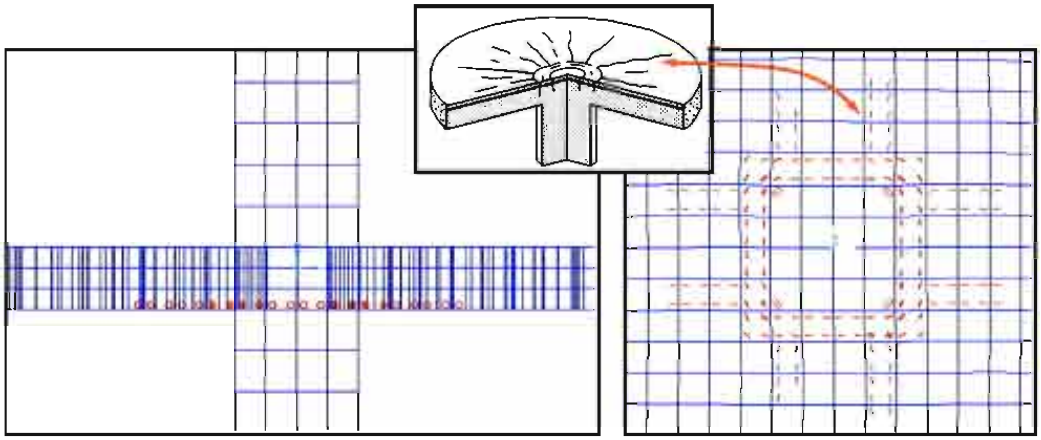

Fig.10: Crack pattern at first loading increments

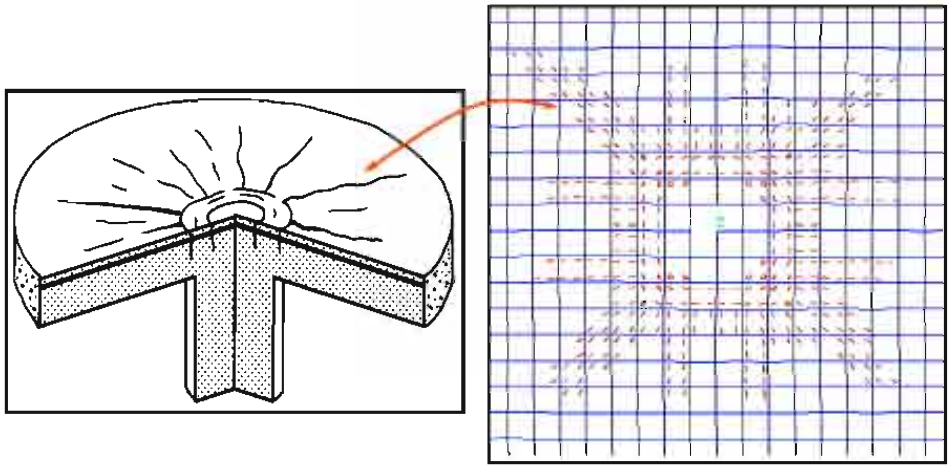

Fig. 11: Crack pattern at middle loading increments

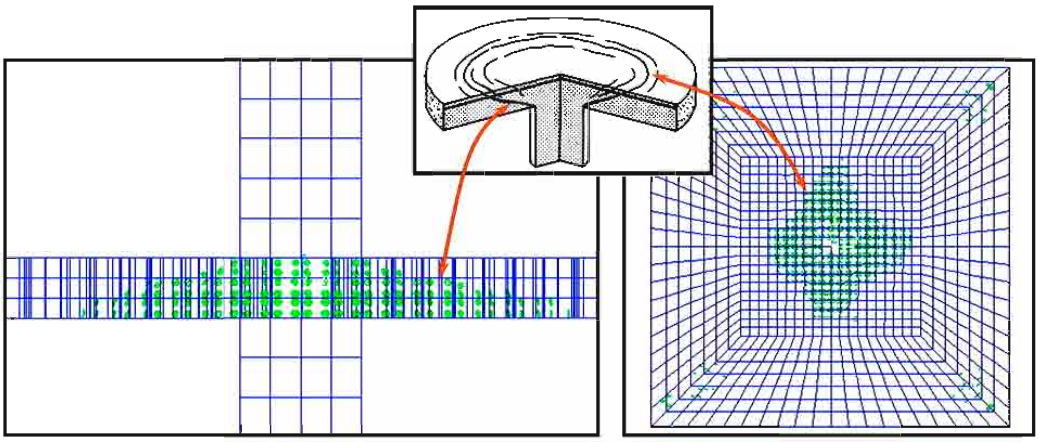

Fig. 12: Crack pattern at period just prior to ultimate load with eliminating radial cracks

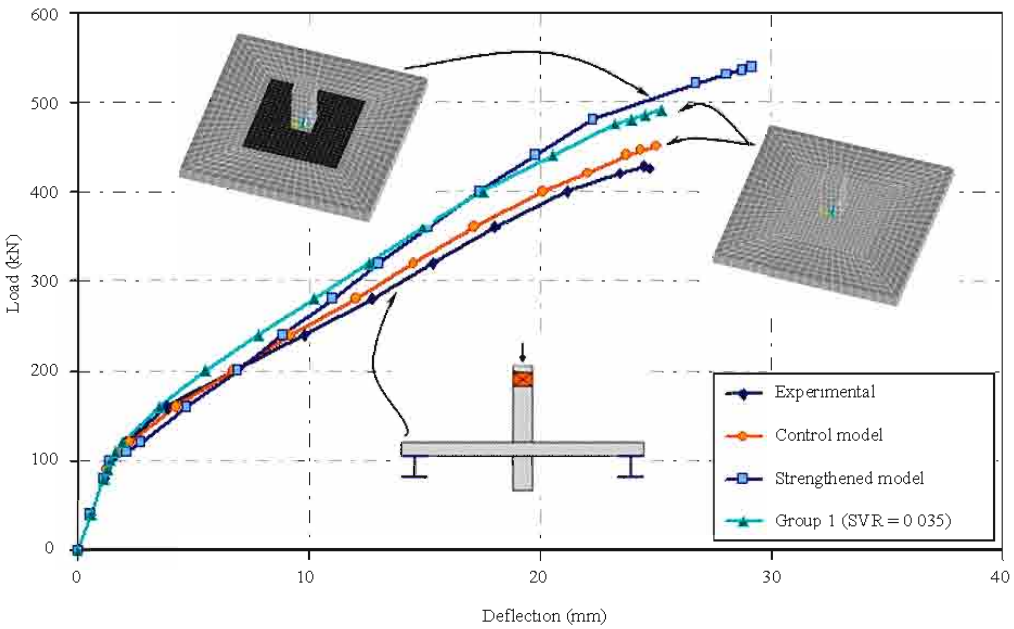

Fig. 13: Comparison of load-deflection curves (SVR= Steel Volume Ratio)

material layers with different orientations and orthotropic material properties in each layer. The element has three degrees of freedom at each node and translations in the nodal x, y and z directions. Nodes of the FRP layered solid elements were connected to those of adjacent concrete solid elements in order to satisfy the perfect bond assumption. The material properties for FRP composites are available at Table 1. By using Solid 46 element, one layer of CFRP with the thickness of 2 mm in two sides of base model in central zone was defined (Fig. 14).

The various thicknesses of the FRP composites create discontinuities, which are not desirable for the finite element analysis. These may develop high stress concentrations at local areas on the models; consequently, when the model is run, the solution may have difficulties in convergence. Therefore, a consistent overall thickness of FRP composite was used in the models to avoid discontinuities. The equivalent overall stiffness of the FRP materials was maintained by making compensating changes in the elastic and shear moduli

Table 1 Summary of material properties for CFRP composites

FRP composite	Elastic modulus (MPa)	Major Poisson's ratio	Tensile strength (MPa)	Shear modulus (MPa)	Thickness of laminate (mm)
CFRP	E_x = 62000	ν_{xy} = 0 22	958	G_{xy} = 3270	1 0
	E_y = 4800	ν_{xz} = 0 22		G_{xz} = 3270	
	E_z = 4800	ν_{yz} = 0 30		G_{yz} = 1860	

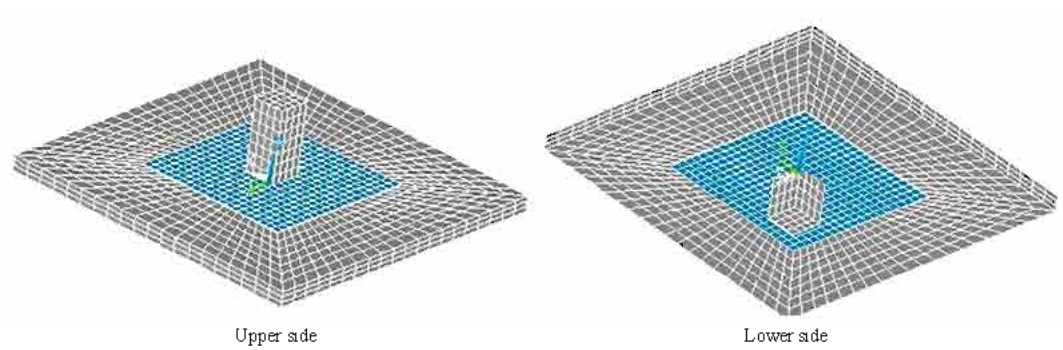

Fig. 14: Slab strengthening model in central zone by using Solid 46 element

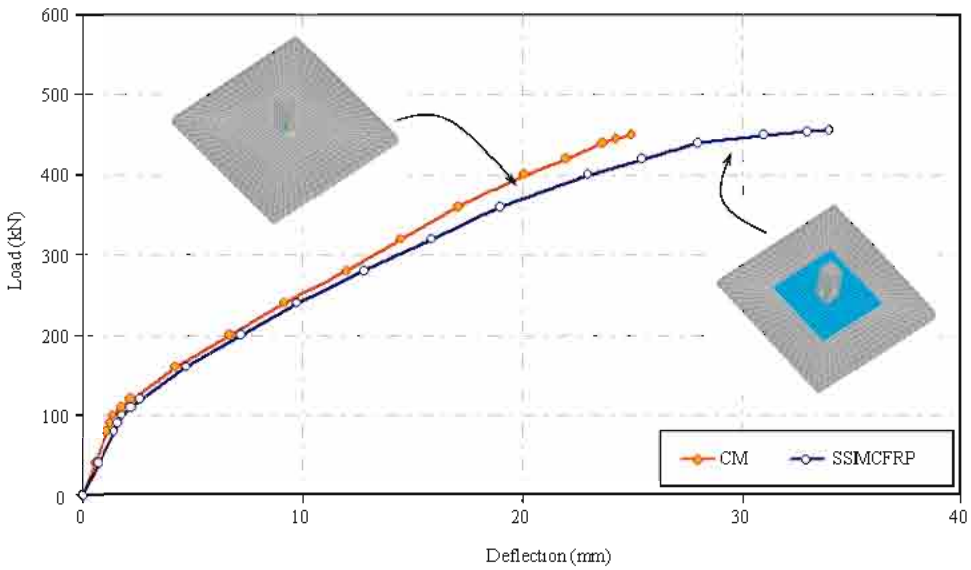

Fig. 15: Comparison of load-deflection curves between Control Model (CM) and Strengthened Slab Model with CFRP (SSMCFRP)

assigned to each FRP layer. For example, if the thickness of an FRP laminate was artificially doubled to maintain a constant overall thickness, the elastic and shear moduli in that material were reduced by 50% to compensate. Note that the relationship between elastic and shear moduli is linear (ANSYS, 2004).

Figure 15 shows the load-deflection curve of the strengthened model using CFRP in comparison with the same curve of control model. According to the curves, it could be derived that curve slope for strengthened model using CFRP is lower than the other curve. Also, the deflection of strengthened model has been increased by 36 percent; while the slab strength has been increased in a low rate. The deflection of strengthened model was 34 mm and the ultimate load reached to 456 kN; while the deflection of basic model was 25 mm and the ultimate load had reached to 449 kN. By considering that in order to increase the ductility and shear strength, it is necessary that the lines of shear cracks should be cut by shear reinforcement, it seems that by applying the shear

studs made of CFRP in the central zone between the CFRP plates, the shear strength and ductility could be increased properly.

CONCLUSIONS

From the discussion of results obtained by testing and numerical modeling, the following conclusions can be drawn:

- The numerical investigations provided good agreement between the predicted and the available test results of the ultimate load and associated deflection.
- It is important to select an appropriate mesh size to meet the requirement of accuracy and computation speed.
- It is necessary to carry out a parametric study and look at the effect of the volume of smeared reinforcement, if the mesh is not uniform. This problem does not occur in the discrete reinforcement modeling.
- The slab model of group I which consisted of the smeared reinforcement throughout the entire slab provides the closest results compared with the experimental test.
- Although the smeared models do give accurate approximations, their behavior is slightly different. The precracking branch of the different curves follows the experimental results very closely. Beyond cracking, the models of group II appear stiffer.
- The smeared crack indicated a crack pattern similar to the experimental specimen.
- 3D finite element model simulated punching shear behavior of the experimental specimen.
- The deflection of strengthened model by using CFRP has been increased by 36%; while the slab strength has been increased in a low rate. The deflection of strengthened model was 34 mm and the ultimate load reached to 456 kN; while the deflection of basic model was 25 mm and the ultimate load had reached to 449 kN.
- Considering the cracking pattern, it seems that by applying the shear studs made of CFRP in the central zone between the CFRP plates, the shear strength and ductility could be increased properly.
- Strengthened model with increasing steel volume ratio in the central zone increased both, the final load and deflection.

REFERENCES

Ajdukiewice, A. and W. Starosolski, 1990. Reinforced-Concrete Slab-Column Structures. Elsevier, New York, USA.

ANSYS., 2004. ANSYS User's Manual Revision 9.0. ANSYS, Inc., United States.

ASCE., 2002. Task Committee on Finite Element Analysis of Reinforced Concrete Structures. State-of-the-Art Report on Finite Element Analysis of Reinforced Concrete, ASCE Special Publications.

Bangash, M.Y.H., 1989. Concrete and Concrete Structures: Numerical Modeling and Applications. Elsevier Science Publishers Ltd., London.

Desayi, P. and H.K. Seshadri, 1997. Punching shear strength of flat slab corner column connections. Part 1. Reinforced Concrete Connections. Struct. Buildings, 122: 10-20.

Dyngeland, T., K. Hoiseth, E. Opheim and A.R. Hole, 1994. Nonlinear Analyses of Reinforced Concrete Members Subjected to Punching Shear. In: Computational Modeling of Concrete Structures, Mang, H., N. Bicanic and R. Borst (Eds.). Innsbruck, pp: 865-873.

Farhey, D.N., M.A. Adin and D.Z. Yankelevsky, 1995. Repaired RC Flat-Slab-Column Sub assemblages under Lateral Loading. JSE, 5: 1710-1720.

FEMA., 1997. FEMA-274 Commentary on the Seismic Rehabilitation of Reinforced Concrete Structures. Federal Emergency Management Agency, Washington DC., pp: 6-18.

Gardner, N.J. and X.Y. Shao, 1996. Punching shear of continuous flat reinforced concrete slabs. ACI Struct. J., 93 (6): 216-228.

Ghali, A. and S. Megally, 2000. Stud shear reinforcement for punching: North American and European Practices. Proceedings of the International Workshop on Punching Shear Capacity of RC Slabs, Kungl Tekniska Hogskolan Institute for Byggkonstruktion, Stockholm, Sweden, pp: 201-209.

Hallgren, M., 1996. Punching shear capacity of reinforced high strength concrete slabs. Royal Institute of Technology, TRITA-BKN. Stockholm, Bull., 23: 107-112.

Hemmaty, Y., 1998. Modeling of the shear force transferred between cracks in reinforced and fiber reinforced concrete structures. Proceedings of the ANSYS Conference Pittsburgh Pennsylvania, 1: 123-138.

Huyse, L., Y. Hemmaty and L. Vandewalle, 1994. Finite element modeling of fiber reinforced concrete beams. Proceedings of the ANSYS Conference, Pittsburgh, Pennsylvania, 2: 72-84.

Kheyroddin, A. and H. Naderpour, 2006. Nonlinear finite element analysis of rc shear walls retrofitted using externally bonded steel plates and FRP sheets. Proceedings of 32th CSCE Annual Conference, 1st International Structural Specialty Conference, Calgary, Alberta, Canada.

Kruger, G., O. Burdet and R. Favre, 1998. Punching tests on rc flat slabs with eccentric loading. 2nd International Ph.D Symposium in Civil Engineering, Budapest, Hongrie, pp: 1-8.

Malvar, L.J., 1992. Punching shear failure of a reinforced concrete pier deck model. ACI Struct. J., 89 (5): 569-576.

Marzouk, H. and Z. Chen, 1993. Finite element analysis of high strength concrete slabs. ACI Struct. J., 90 (5): 505-513.

Marzouk, H. and D. Jiang, 1996. Finite element evaluation of shear enhancement of high strength concrete plates. ACI Struct. J., 93 (6): 667-673.

Menétrey, Ph., 1994. Numerical analysis of punching failure in reinforced concrete structures. Ph.D Thesis, Lausanne.

Nilson, A.H., D. Darwin and Ch.W. Dolan, 2003. Design of Concrete Structures. 13th Edn. McGraw Hill, New York, USA.

Polak, M., 1998. Modeling punching shear of reinforce concrete slabs using layered finite elements. ACI Struct. J., 95 (1): 71-80.

Triantafillou, T.C., 2003. Seismic retrofitting using bonded fiber reinforced polymers (FRP). University of Patras, Department of Civil Engineering, Patras GR-26500.

Vidosa, F.G., M.D. Kostsovos and M.N. Pavlovic, 1991. Three-dimensional nonlinear finite element model for structural concrete. Proceedings of the Institution of Civil Engineers Part 2 Research and Theory, 91: 517-560.